Discriminative EEG Feature Extraction Using the Adaptive Synchrosqueezing Wavelet Transform for Epileptic Seizure Detection

NON−PEER-REVIEWED PREPRINT

Arpish R. Solanki
Ahmedabad, India

ABSTRACT

This study investigated using the Adaptive Synchrosqueezing Wavelet Transform (ASST) for feature extraction in EEG-based epileptic seizure detection. Traditional time-frequency methods, notably the Continuous Wavelet Transform (CWT) and Short-Time Fourier Transform (STFT), were used to extract similar features and compared against ASST for seizure detection performance. Classification experiments using Support Vector Machines (SVM), Random Forest (RF), and K-Nearest Neighbors (KNN) showed that ASST-derived features led to strong classification performance for distinguishing seizure and non-seizure EEG segments. The Random Forest classifier achieved the best performance using ASST features, with an accuracy of 99.09%, an F1-score of 97.71%, and an AUC-ROC of 0.9990 after applying class balancing with SMOTE. The results showed that ASST achieved slightly higher classification performance compared to STFT and CWT, suggesting its potential as an effective and adaptive tool for non-stationary EEG analysis in seizure detection.

Keywords EEG · Epileptic Seizure Detection · Time-Frequency Analysis · Feature Extraction · Machine Learning

1 Introduction

Epilepsy is one of the most common chronic neurological conditions, affecting an estimated 4 to 10 per 1,000 people worldwide, with up to 8% of individuals having at least one seizure during their lifetime [1]. Epilepsy is characterized by recurrent seizures and transient spikes of abnormal electrical activity in the brain. It has a severe effect on quality of life and imposes substantial personal, social, and economic burdens. The risk of early death of individuals with epilepsy is up to three times higher than for the general population [2], which emphasizes the importance of efficient seizure detection and management techniques.

A key tool for diagnosing and monitoring epilepsy is electroencephalography, or EEG [3]. Practitioners can detect epileptiform patterns, such as spikes, sharp waves, and rhythmic discharges, that are suggestive of seizure activity by using scalp electrodes to non-invasively record the brain's electrical activity. However, EEG's diagnostic and predictive ability can be dependent on its capability to extract useful information from complex and non-stationary signals [4].

EEG signals change dynamically throughout time due to the brain's constantly changing activity, and seizure-related patterns frequently include brief, high-amplitude transients or evolving rhythmic discharges, depending on the type of seizure. Traditional time-domain features, such as mean, median, and variance, among others [5], and frequency-domain techniques, such as the Fourier Transform, provide partial insights. Consequently, temporal and spectral information captured by time-frequency representations (TFRs) are now commonly used methods in EEG research [6].

The Wavelet Transform (WT) and the Short-Time Fourier Transform (STFT) are two of the most often utilized TFR techniques [7]. Although STFT analyzes frequency content across time by segmenting signals into fixed-size windows, it has a fundamental trade-off between frequency resolution and time. Narrow windows increase temporal resolution but reduce frequency resolution, whereas wide windows do the opposite [8]. Wavelet-based approaches, such as the CWT, promote adaptability by enabling multiresolution analysis using scalable wavelet functions. The mother wavelet

selection still has a significant impact on the result, though [9]. In addition, these techniques can give representations with signal energy dispersed across multiple frequencies.

Time and frequency reassignments were introduced to improve energy concentration in the time-frequency plane. SST, a type of reassignment method based on CWT, was introduced by Daubechies et al. in [10] and further developed in [11]. SST improves energy concentration and separates multicomponent signals to produce a TF representation with better energy concentration and sharper resolution compared to the original WT. It acts as a reallocation method, by estimating the instantaneous frequency of signal components at each point in the WT's time-scale plane and then "squeezing" or reassigning the WT coefficients to these estimated frequencies in the TF plane.

SST has been applied in various EEG-related applications. Yousif and Ozturk [12] used SST to obtain time-frequency representation matrices of EEG signals for motor imagery (MI) classification in BCI. They used principal component analysis for dimension reduction and feature extraction, followed by support vector machine (SVM) classification. Karakullukcu and Yilmaz [13] used SST (particularly, the Fourier-based synchrosqueezing transform, or FSST) to extract features for distinguishing between resting and motor imagery states in an EEG-based BCI. They used FSST with singular value decomposition (SVD) for feature selection and support vector machines for classification. Wang et al. [14] compared SST to other time-frequency analysis methods (Hilbert-Huang Transform and Morlet Wavelet Transform) to analyze TMS-evoked EEG oscillations.

Cura and Akan [15] used time-frequency representations of EEG signals to detect epileptic seizures. They extracted features from these representations and used different machine learning classifiers for classification. Ozdemir et al. [16] used Fourier-based SST in conjunction with a Convolutional Neural Network (CNN) for epileptic seizure detection and prediction. Amiri et al. [17] combined sparse common spatial pattern and adaptive short-time Fourier transform-based synchrosqueezing transform for automatic epileptic seizure detection in EEG signals.

Marchi et al. [18] presented the Adaptive Synchrosqueezing Wavelet Transform (ASST), which dynamically improves time-frequency representations based on local signal properties. ASST extends the traditional Synchrosqueezing Transform (SST) by using adaptive reassignment rules and iterative refinement processes to increase wavelet-based representation resolution. ASST seeks to improve TF resolution efficiently while reducing computational load by iteratively estimating signal energy across frequency bands within data batches and reallocating a limited number of analysis frequencies to regions of interest. Despite its theoretical benefits, ASST is still underexplored in the area of Brain-Computer Interfaces (BCIs) and seizure detection.

Time-frequency methods like SST improve energy localization by concentrating spectral content near instantaneous frequencies which can improve the visibility of short-lived, non stationary events such as spikes or evolving rhythmic discharges seen in seizures. The ASST extends this principle by introducing computational adaptivity, which allows sharper and more informative representations while effectively focusing on the most relevant regions of the EEG.

To the best of the author's knowledge, this study is the first application of ASST to neurological signal analysis, including epileptic seizure detection from EEG. This study explores the use of ASST to extract features from seizure EEG signals and compares its performance to other common approaches such as STFT and CWT. The explored pipeline extracts multiple spectral and statistical features from ASST-based time-frequency representations. Classification is done using a variety of machine learning classifiers, such as SVM, Random Forest, and KNN.

The remainder of this paper is organized as follows: Section 2 outlines the methodology, including dataset details, feature extraction using the Adaptive Synchrosqueezing Wavelet Transform (ASST), and the classification pipeline. Section 3 presents the experimental results, including feature separability and classification performance. Section 4 discusses the implications of the findings. Finally, Section 5 concludes the study.

2 Methods

2.1 Dataset Description

The dataset used in this study was the Epileptic Seizure Recognition Dataset, originally from the UCI Machine Learning Repository, and obtained via Kaggle. This dataset consisted of preprocessed EEG recordings from 500 individuals, where each individual's brain activity was recorded for 23.6 seconds. The original recordings were sampled into 4097 data points per subject, representing the EEG signal at different time points. These EEG signals were collected to classify seizure activity and distinguish it from non-seizure states.

2.1.1 Segmenting and Labeling EEG Data

The dataset used in this study was a preprocessed and segmented version of a publicly available Epileptic Seizure Recognition Dataset. Each original 23.6-second recording was reshaped into 1-second segments of 178 samples, resulting in 11,500 labeled segments [19]. Only class 1 segments represent epileptic seizure activity, while classes 2 through 5 represent non-seizure states. No further preprocessing was applied beyond what was provided. Each 1-second EEG segment was used as input for time-frequency feature extraction via the ASST.

The target variable (column 179 in the dataset) represented different brain states. There were five labels:

- Seizure Activity (Class 1): EEG recordings that contain seizure activity.
- Tumor Region EEG (Class 2): EEG signals recorded from the tumor-affected brain region.
- Healthy Brain (Class 3): EEG signals recorded from a non-affected region of the brain in tumor patients.
- Eyes Closed (Class 4): EEG signals recorded from individuals with their eyes closed.
- Eyes Open (Class 5): EEG signals recorded from individuals with their eyes open.

2.2 Adaptive Synchrosqueezing Wavelet Transform (ASST) for Feature Extraction

The Adaptive Synchrosqueezing Wavelet Transform (ASST) is a time-frequency analysis technique that extends the classical Synchrosqueezing Wavelet Transform (SST) by introducing a dynamic, energy-based frequency discretization strategy. It is designed to improve time-frequency resolution while reducing computational cost, which makes it suitable for real-time and resource-constrained applications.

At its core, ASST operates in the same framework as SST, it begins by computing the Continuous Wavelet Transform (CWT) of a signal $s(t)$ using a complex mother wavelet $\psi(t)$:

$$W_s(a,b) = \int s(t)\, a^{-1/2}\, \psi^* \left(\frac{t-b}{a} \right) dt$$

From this representation, the instantaneous frequency is estimated using the derivative of the phase:

$$\omega_s(a,b) = \Re \left\{ -i \cdot \frac{1}{W_s(a,b)} \cdot \frac{\partial W_s(a,b)}{\partial b} \right\}$$

These frequency estimates are used to reassign the energy of the wavelet coefficients into sharper ridges in the time-frequency plane via the synchrosqueezing operation.

Unlike SST, which performs this reassignment on a fixed, uniformly spaced frequency grid, ASST introduces an adaptive grid $\{w_k\}$ that is iteratively refined based on the energy distribution of the signal. The energy within each frequency bin over a frame of the signal is computed as:

$$E_N(w_k) = \sum_n |S_s(w_k, b_n)|^2 \cdot \Delta\omega_k$$

and normalized:

$$\hat{E}_N(w_k) = \frac{E_N(w_k)}{\sum_j E_N(w_j)}$$

The normalized energy $\hat{E}_N(w_k)$ guides the reallocation of frequency bins to regions of interest using either:

- Proportional distribution, where bins are assigned in proportion to energy,
- Or thresholding, where low-energy bins are discarded and reassigned to more informative regions.

Once the adaptive grid is formed, the synchrosqueezing operation is recomputed over this updated frequency set.

2.3 Feature Extraction Using ASST

EEG signals were transformed into the time-frequency domain using the ASST, implemented with a threshold-based reassignment strategy set to 1/30 and Out-of-the-Loop (OTL) synchrosqueezing. The ASST was configured to span 0.5–80 Hz over 159 linearly spaced frequency bins. From the resulting ASST energy distribution $S(t, f)$, spectral features were extracted, including peak frequency (maximum energy), mean frequency (energy-weighted average), and spectral entropy. Band energy features were computed by summing energy within conventional EEG frequency bands (delta, theta, alpha, beta, gamma). In addition, statistical features such as mobility, complexity, skewness, and kurtosis were extracted directly from the raw EEG time series to capture signal morphology and variability.

To establish a fair comparison with the ASST-based pipeline, identical features were extracted from the time-frequency representations obtained using Short-Time Fourier Transform (STFT) and Continuous Wavelet Transform (CWT). The CWT was implemented using the complex Morlet (CMOR) wavelet. For both methods, this study computed peak frequency, mean frequency, spectral entropy, and band energy across standard EEG frequency ranges. These were calculated by summing the squared magnitude of the time-frequency representation across time and integrating within the respective frequency bands, consistent with the ASST feature extraction strategy. Additionally, statistical features such as mobility, complexity, skewness, and kurtosis were derived directly from the raw EEG signal for all methods.

2.3.1 Extracted ASST Features

From the ASST representation, the following spectral and statistical features were computed:

Spectral Features:

Peak Frequency (Hz): The frequency with the highest energy concentration, defined as:

$$f_{\text{peak}} = \arg\max_f \sum_t |S(t, f)^2|$$

Mean Frequency (Hz): The energy-weighted average frequency:

$$f_{\text{mean}} = \frac{\sum_f f \sum_t |S(t, f)|^2}{\sum_f \sum_t |S(t, f)|^2}$$

Spectral Entropy: A measure of signal disorder, defined as:

$$H = -\sum_f P(f) \log_2 P(f), \quad P(f) = \frac{\sum_t |S(t, f)|^2}{\sum_f \sum_t |S(t, f)|^2}$$

where $S(t, f)$ represents the energy magnitude at time t and frequency f.

Band Energy Features:

The energy in specific frequency bands was extracted by integrating energy over predefined ranges:

- Delta (0.5–4 Hz)
- Theta (4–8 Hz)
- Alpha (8–12 Hz)
- Beta (12–30 Hz)
- Gamma (30–80 Hz)

Statistical Features

In addition to ASST-based features, statistical measures were extracted from the raw EEG signal to quantify its distribution and variability:

Mobility: Measures signal smoothness, given by:

$$M = \frac{\sigma_{\Delta x}}{\sigma_x}$$

where σ_x is the standard deviation of the signal and $\sigma_{\Delta x}$ is the standard deviation of its first derivative.

Complexity: Evaluates the degree of variation in signal mobility, defined as:

$$C = \frac{\sigma_{\Delta^2 x}}{\sigma_{\Delta x}}$$

where:

- σ_x is the standard deviation of the signal,
- $\sigma_{\Delta x}$ is the standard deviation of the first derivative,
- $\sigma_{\Delta^2 x}$ is the standard deviation of the second derivative.

Skewness: Measures signal asymmetry:

$$S = \frac{E[(x-\mu)^3]}{\sigma^3}$$

Kurtosis: Assesses the presence of outliers or extreme values in the signal distribution:

$$K = \frac{E[(x-\mu)^4]}{\sigma^4}$$

where:

- $E[\cdot]$ denotes the expectation (mean),
- μ is the mean of the signal,
- σ is the standard deviation of the signal.

2.4 Classification Pipeline

Extracted features were prepared for binary classification by relabeling class 1 as "Seizure" and grouping classes 2–5 as "Non-Seizure." An 80/20 stratified train-test split was applied, and features were standardized using z-score normalization. Three classifiers Random Forest, Support Vector Machine (RBF kernel), and K-Nearest Neighbors were trained using both the original imbalanced training data and a balanced version generated with SMOTE. Model performance was evaluated on the untouched test set using accuracy, precision, recall, F1-score, and AUC-ROC. To evaluate the robustness and generalizability of ASST-based features, identical classification procedures were applied to features extracted from Short-Time Fourier Transform (STFT) and Continuous Wavelet Transform (CWT) representations.

This study used several exploratory tools to interpret and visualize the separability of extracted features. T-distributed Stochastic Neighbor Embedding (t-SNE) was used to project the high-dimensional feature vectors into a 2D space, for qualitative visualization of class separation across different time-frequency methods. Kernel Density Estimation (KDE) plots were generated for individual features to inspect seizure and non-seizure class-wise distributions. Additionally, Cohen's *d* was computed for each feature to quantify its effect size between the seizure and non-seizure classes.

2.4.1 Implementation Details

The Adaptive Synchrosqueezing Wavelet Transform (ASST) was applied using the official Python package provided by Marchi et al. [21], which is publicly available on GitHub. Time-frequency feature extraction was performed using the adaptivesswt library for ASST, pywt for Continuous Wavelet Transform (CWT), and scipy.signal for Short-Time Fourier Transform (STFT). Statistical descriptors, including entropy, skewness, and kurtosis, were computed using functions from the scipy.stats module. Machine learning models were developed using the scikit-learn library, which provided tools for classification (SVM, Random Forest, KNN), evaluation metrics (accuracy, precision, recall, F1-score, AUC), and dimensionality reduction (t-SNE). To address class imbalance, the SMOTE algorithm was applied using the imblearn package. Data visualization, including KDE plots and t-SNE projections, was carried out using seaborn and

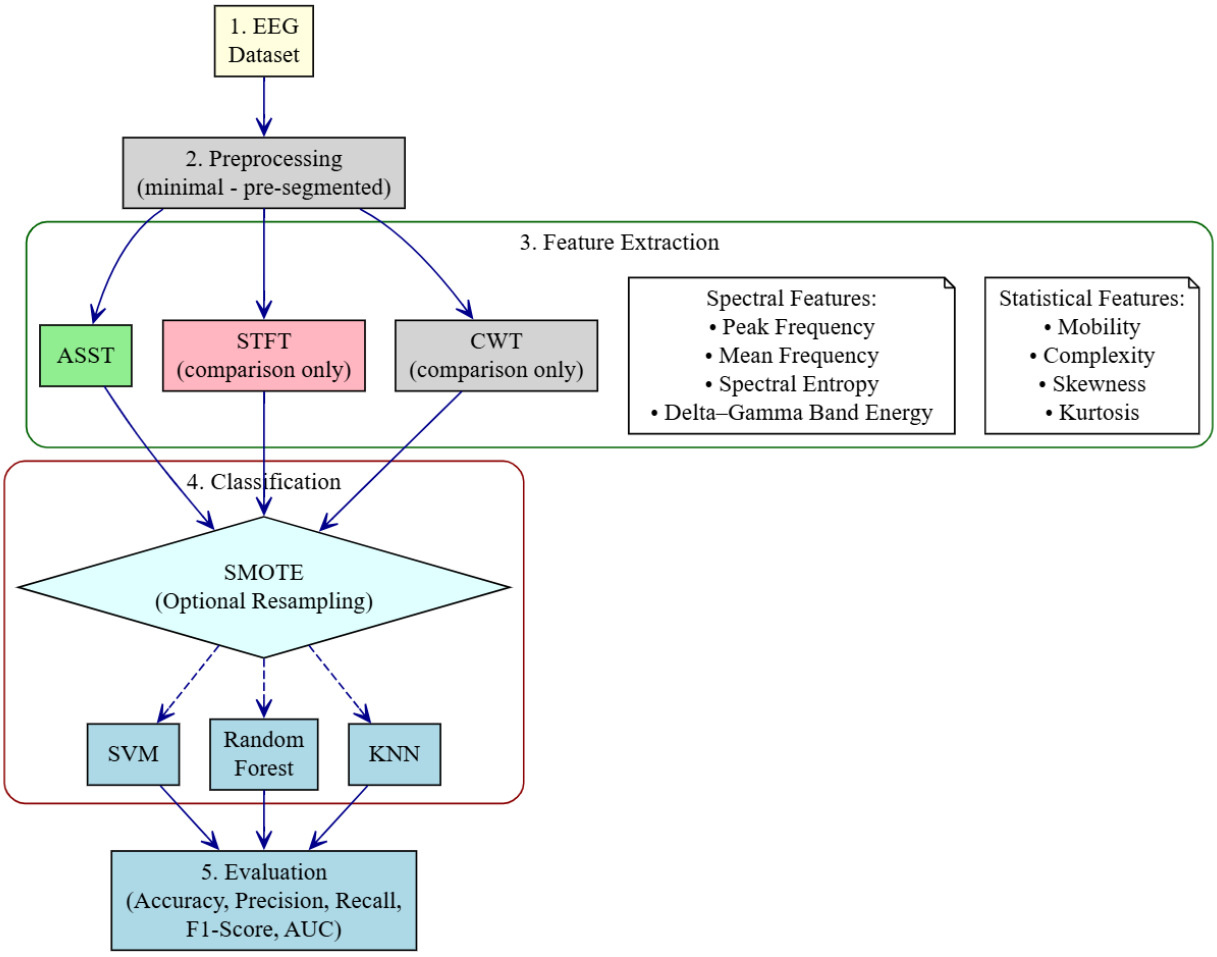

Figure 1: Pipeline for EEG-based seizure detection.

matplotlib. This software environment supported the reproducible development and evaluation of all feature extraction and classification pipelines in the study.

3 Results

3.1 Feature Separability and Visualization

This study used t-SNE to reduce the dimensionality of the retrieved features to assess their discriminative power. Feature clusters are visualized in a reduced 2D space in Figure 2. The observed separation between seizure and non-seizure instances showed that ASST-based features had discriminative power, comparable with traditional methods.

In addition, Cohen's d was calculated for all features to determine their ability to distinguish between seizure and non-seizure states. Table 1 shows the top five most separable features, ranked by effect size. Gamma_energy had the largest effect size, suggesting that it plays an important role in distinguishing seizure from non-seizure states.

Figure 3 displays KDE plots for ASST-extracted features and their distribution across seizure and non-seizure classes. These visualizations offer information on the feature separability, with differences in spectral energy, frequency characteristics, and statistical characteristics between the two conditions. Band energy features have distinctive density distributions, which suggests that they may be useful for seizure classification.

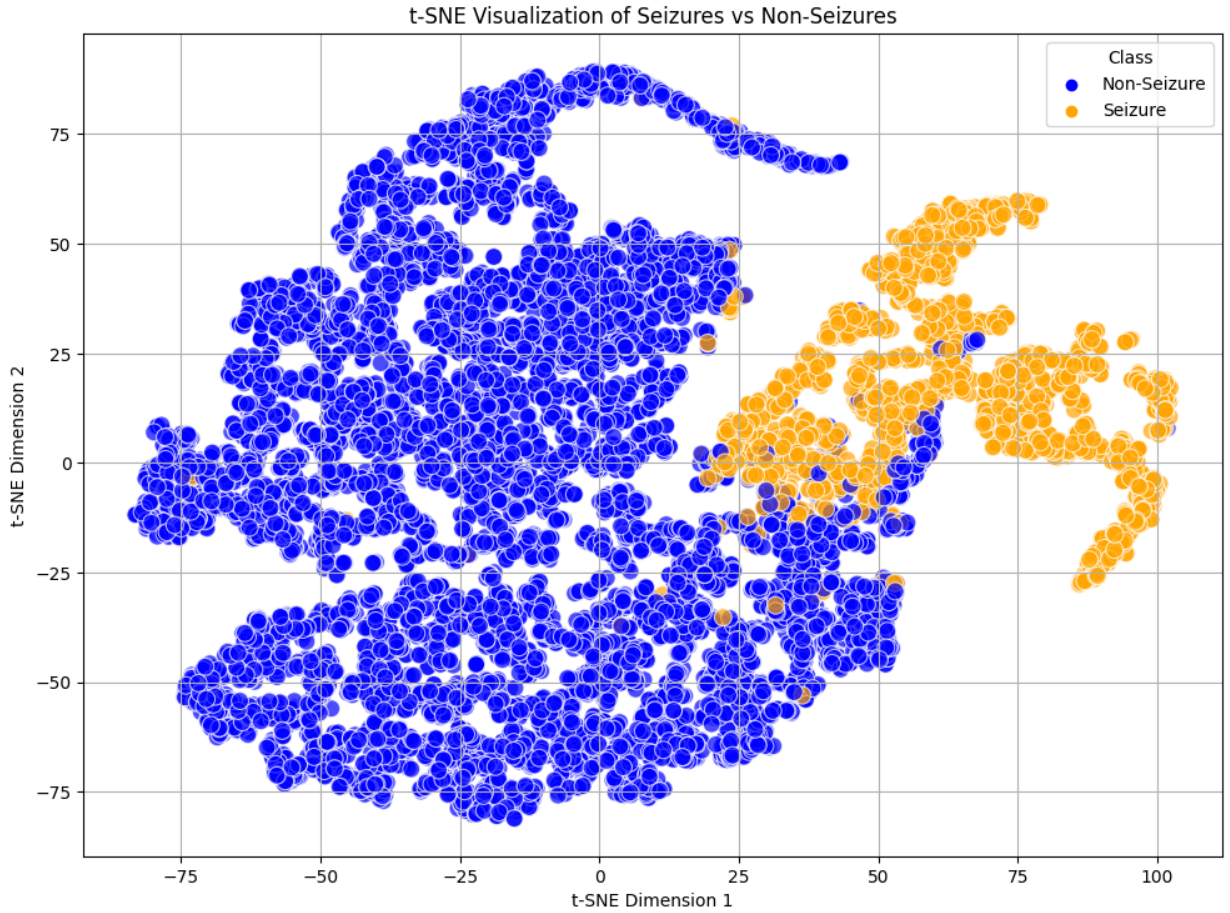

Figure 2: Two-dimensional t-SNE projection of ASST-extracted features, illustrating the clustering of seizure (yellow) and non-seizure (blue) EEG instances.

Rank	Feature	Cohen's d
1	Gamma_energy	1.3515
2	Beta_energy	1.1625
3	Delta_energy	0.9927
4	Theta_energy	0.8508
5	Alpha_energy	0.8312

Table 1: Top five features ranked by their Cohen's d effect sizes.

3.2 Classification Performance

This section presents the classification results for seizure detection with ASST-based features, along with results from other methods' features. The performance of three machine learning classifiers Random Forest (RF), Support Vector Machine (SVM), and K-Nearest Neighbors (KNN) was evaluated both before and after applying Synthetic Minority Over-sampling Technique (SMOTE) to address class imbalance.

3.2.1 Classification Performance Before SMOTE

Before applying SMOTE, the dataset had a large class imbalance, with 9200 non-seizure instances much outnumbering 2300 seizure instances. This mismatch frequently causes classification models to favor the majority class, potentially leading to inferior seizure detection performance. For the ASST, the RF classifier achieved highest accuracy (98.96%), while maintaining strong precision (98.23%) and recall (96.52%) and a high AUC-ROC score of 0.9991. The SVM followed closely with 98.39% accuracy, though its seizure recall (95.43%) was slightly lower. Meanwhile, KNN fared

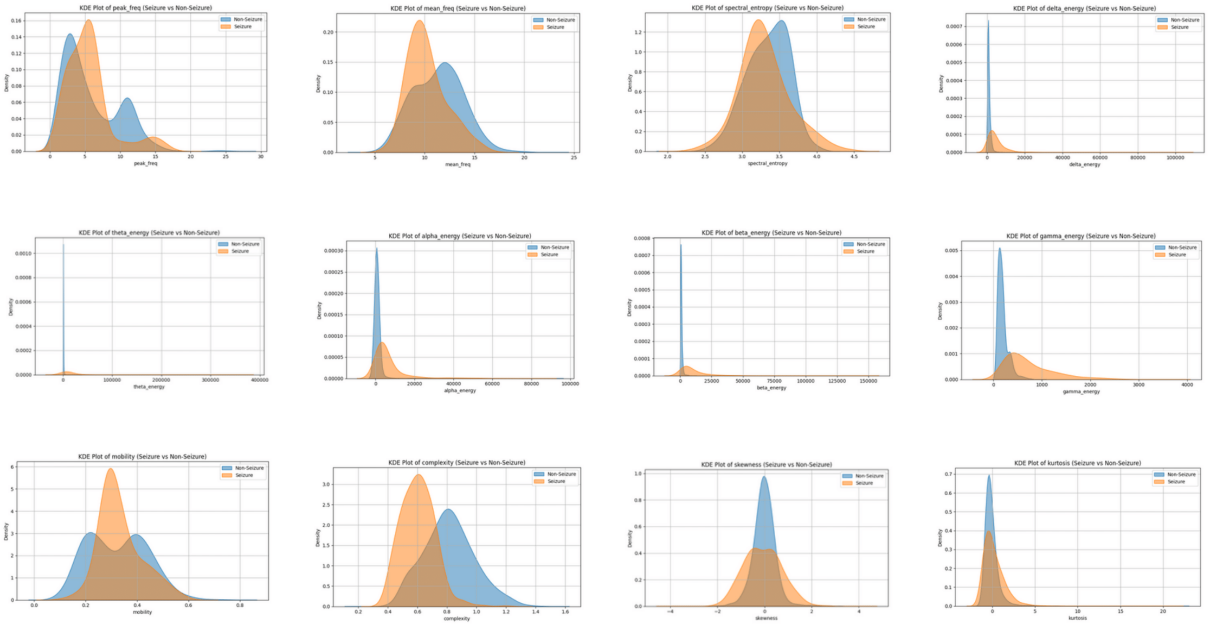

Figure 3: Kernel Density Estimation (KDE) plots of ASST-derived features for seizure (orange) and non-seizure (blue) EEG segments, illustrating feature distributions. The features, shown in order from left to right and top to bottom, are: Peak Frequency, Mean Frequency, Spectral Entropy, Delta Band Energy, Theta Band Energy, Alpha Band Energy, Beta Band Energy, Gamma Band Energy, Mobility, Complexity, Skewness, and Kurtosis.

well, reaching 98.52% accuracy and 98.41% precision, while its recall (94.13%) was slightly reduced. Overall, as Table 2 shows, RF, SVM and KNN performed well in classification before SMOTE was applied.

Classifier	Accuracy	Precision	Recall	F1 Score	AUC-ROC
Random Forest	98.96%	98.23%	96.52%	97.37%	0.9991
SVM	98.39%	96.48%	95.43%	95.96%	0.9987
K-Nearest Neighbors	98.52%	98.41%	94.13%	96.22%	0.9909

Table 2: Classification results using features extracted with Adaptive Synchrosqueezing Wavelet Transform (ASST) before SMOTE.

CWT Classification Results

The Continuous Wavelet Transform (CWT) was used to extract the same features from the same EEG dataset for comparison. The classification results are shown in Table 3.

Classifier	Accuracy	Precision	Recall	F1 Score	AUC-ROC
Random Forest	98.91%	97.59%	96.96%	97.27%	0.9991
SVM	98.35%	97.52%	94.13%	95.80%	0.9981
K-Nearest Neighbors	98.26%	97.73%	93.48%	95.56%	0.9874

Table 3: Classification results using features extracted with Continuous Wavelet Transform (CWT) before SMOTE.

STFT Classification Results

The Short-Time Fourier Transform (STFT) was used on the dataset to extract the same set of features. The classification results are provided in Table 4.

3.2.2 Classification Performance After SMOTE

To address class imbalance, SMOTE was applied to ensure an equal representation of seizure and non-seizure instances. As shown in Table 5, this balancing improved seizure detection recall while maintaining high precision across classifiers.

Model	Accuracy	Precision	Recall	F1 Score	AUC-ROC
Random Forest	98.65%	96.94%	96.30%	96.62%	0.9991
SVM	98.61%	97.14%	95.87%	96.50%	0.9986
K-Nearest Neighbors	98.35%	97.31%	94.35%	95.81%	0.9886

Table 4: Classification results using features extracted with Short-Time Fourier Transform (STFT) before SMOTE.

Using ASST-derived features, the RF classifier achieved a slight improvement, reaching 99.09% accuracy with an increased recall of 97.61% and a consistently high AUC-ROC of 0.9990. The SVM exhibited a significant recall boost (98.04%), though its precision slightly declined due to increased sensitivity to seizure cases, resulting in an overall accuracy of 98.13%. Similarly, the KNN classifier saw recall improvements (96.52%), achieving an accuracy of 98.04%. Comparing alternative methods, CWT features led to an RF accuracy of 98.91%, with an exceptional AUC-ROC of 0.9992, while SVM reached 98.22% accuracy with strong recall (97.17%). The STFT produced comparable results, with RF achieving 98.78% accuracy and an AUC-ROC of 0.9990, while SVM maintained a high recall of 98.26%.

Feature Set	Classifier	Accuracy	Precision	Recall	F1 Score	AUC-ROC
ASST	Random Forest	99.09%	97.82%	97.61%	97.71%	0.9990
	SVM	98.13%	92.99%	98.04%	95.45%	0.9981
	KNN	98.04%	93.87%	96.52%	95.18%	0.9907
CWT	Random Forest	98.91%	96.77%	97.83%	97.30%	0.9992
	SVM	98.22%	94.11%	97.17%	95.61%	0.9970
	KNN	97.74%	92.86%	96.09%	94.44%	0.9860
STFT	Random Forest	98.78%	96.35%	97.61%	96.98%	0.9990
	SVM	98.48%	94.36%	98.26%	96.27%	0.9982
	KNN	98.00%	92.77%	97.61%	95.13%	0.9891

Table 5: Classification results for ASST, CWT, and STFT features after SMOTE balancing.

4 Discussion

This study explored the use of Marchi et al.'s [18] Adaptive Synchrosqueezing Wavelet Transform (ASST), a time-frequency analysis technique, for EEG-based epileptic seizure detection. The classification results show that seizure and non-seizure events can be effectively distinguished using features derived from ASST. In terms of accuracy and overall classification performance, ASST performed slightly better than CWT and STFT. These findings confirm the discriminative efficacy of ASST-derived features in seizure detection. The Random Forest model delivered the best overall performance out of all the classifiers evaluated, with an accuracy of 99.09%, F1-score of 97.61%, and ROC-AUC of 0.9990. This reflects a good balance between sensitivity and specificity, with few misclassifications. The Support Vector Machine (SVM) and K-Nearest Neighbors (KNN) classifiers likewise produced excellent results. The consistently high performance across all models suggests robust generalization and stable classification across seizure and non-seizure classes.

ASST's slightly better performance across assessment measures can be attributed to its adaptive and iterative reassignment framework, which allows for more precise signal energy localization in the time-frequency domain. ASST dynamically adapts to the signal's local properties [18], [27]. This adaptivity results in a higher concentration of spectral energy near the instantaneous frequencies. ASST's properties improve the clarity of transient and non-stationary patterns present in EEG data, which allows the extraction of more discriminatory features. Overall, ASST's structural adaptivity provides a meaningful advantage over traditional methods, particularly in contexts that demand high temporal and spectral precision.

However, there are some drawbacks to these benefits. Since ASST extends CWT with synchrosqueezing and adaptive reassignment steps, each requiring multiple passes over the signal, it can incur higher computational costs than traditional TFR methods such as STFT or CWT alone [18]. This makes it more computationally demanding when used with larger EEG recordings or in real-time settings. Furthermore, the accuracy was comparable for all methods. This implies that STFT or CWT may still be sufficient for tasks like simple signal visualization where interpretability or computational efficiency are more important than resolution.

4.1 Study Limitations and Future Directions

While the study showed promising results, several limitations should be acknowledged. First, the analysis was performed on the UCI Epileptic Seizure Recognition dataset that is commonly used in seizure detection research and has been shown to have relatively good classification accuracies [28]–[30]. This might not accurately represent the noise and variability seen in real-world clinical EEG recordings. Future research might include evaluating performance on different datasets.

Second, due to the absence of subject labels, this study does not explore inter-patient variability. Although this does not impact the primary purpose of this study, future work could examine subject-specific adaptation or generalization using datasets with richer metadata. Additional research could also investigate the physiological interpretability of the features.

While this study focused on the application of ASST for EEG-based seizure detection, ASST, like STFT and CWT, is a versatile time-frequency analysis method. Future studies could explore its use in other areas involving non-stationary signal analysis, such as in other biomedical signal processing domains.

5 Conclusion

In conclusion, this study demonstrated the effectiveness of the Adaptive Synchrosqueezing Wavelet Transform (ASST) for feature extraction in EEG-based epileptic seizure detection. ASST-derived features allowed for reliable differentiation between seizure and non-seizure EEG segments and achieved slightly higher classification performance than conventional time-frequency methods such as STFT and CWT. Although ASST introduces additional computational complexity, its superior spectral concentration and discriminative feature extraction make it a promising option for advanced EEG analysis and diagnostic support in epilepsy. Future work may explore its application in real-time systems and broader clinical contexts.

References

[1] Z. Chen, M. J. Brodie, D. Ding, and P. Kwan, "Editorial: Epidemiology of epilepsy and seizures," *Frontiers in Epidemiology*, vol. 3, Aug. 2023. DOI: 10.3389/fepid.2023.1273163. [Online]. Available: https://doi.org/10.3389/fepid.2023.1273163.

[2] W. H. O. WHO, *Epilepsy*, Feb. 2024. [Online]. Available: https://www.who.int/news-room/fact-sheets/detail/epilepsy.

[3] S. R. Benbadis, S. Beniczky, E. Bertram, S. MacIver, and S. L. Moshé, "The role of EEG in patients with suspected epilepsy," *Epileptic Disorders*, vol. 22, no. 2, pp. 143–155, Apr. 2020. DOI: 10.1684/epd.2020.1151. [Online]. Available: https://doi.org/10.1684/epd.2020.1151.

[4] M. Tveter, T. Tveitstøl, C. Hatlestad-Hall, *et al.*, "Advancing EEG prediction with deep learning and uncertainty estimation," *Brain Informatics*, vol. 11, no. 1, Oct. 2024. DOI: 10.1186/s40708-024-00239-6. [Online]. Available: https://doi.org/10.1186/s40708-024-00239-6.

[5] I. Stancin, M. Cifrek, and A. Jovic, "A review of EEG signal features and their application in driver drowsiness detection systems," *Sensors*, vol. 21, no. 11, p. 3786, May 2021. DOI: 10.3390/s21113786. [Online]. Available: https://www.ncbi.nlm.nih.gov/pmc/articles/PMC8198610/.

[6] S. Morales and M. E. Bowers, "Time-frequency analysis methods and their application in developmental EEG data," *Developmental Cognitive Neuroscience*, vol. 54, p. 101 067, Jan. 2022. DOI: 10.1016/j.dcn.2022.101067. [Online]. Available: https://doi.org/10.1016/j.dcn.2022.101067.

[7] Z. Zhang, *Spectral and Time-Frequency Analysis*. Jan. 2019, pp. 89–116. DOI: 10.1007/978-981-13-9113-2\{_}6. [Online]. Available: https://doi.org/10.1007/978-981-13-9113-2_6.

[8] K. Feng, J. Cui, H. Dang, *et al.*, "Investigation of a Signal Demodulation Method based on Wavelet Transformation for OFDR to Enhance Its Distributed Sensing Performance," *Sensors*, vol. 19, no. 13, p. 2850, Jun. 2019. DOI: 10.3390/s19132850. [Online]. Available: https://doi.org/10.3390/s19132850.

[9] E. M. Shalby, A. Y. Abdelaziz, E. S. Ahmed, and B. A.-E. Rashad, "A comprehensive guide to selecting suitable wavelet decomposition level and functions in discrete wavelet transform for fault detection in distribution networks," *Scientific Reports*, vol. 15, no. 1, Jan. 2025. DOI: 10.1038/s41598-024-82025-2. [Online]. Available: https://www.nature.com/articles/s41598-024-82025-2.

[10] I. Daubechies and S. Maes, *A nonlinear squeezing of the continuous Wavelet transform based on auditory nerve models*. Nov. 1996, pp. 527–546. DOI: 10.1201/9780203734032-20. [Online]. Available: https://doi.org/10.1201/9780203734032-20.

[11] I. Daubechies, J. Lu, and H.-T. Wu, "Synchrosqueezed wavelet transforms: An empirical mode decomposition-like tool," *Applied and Computational Harmonic Analysis*, vol. 30, no. 2, pp. 243–261, Aug. 2010. DOI: 10.1016/j.acha.2010.08.002. [Online]. Available: https://doi.org/10.1016/j.acha.2010.08.002.

[12] M. A. A. Yousif and M. Ozturk, "Motor Imagery BCI Classification Using Synchrosqueezing Transform," Jul. 2023, pp. 1–4. DOI: 10.1109/siu59756.2023.10223986. [Online]. Available: https://doi.org/10.1109/siu59756.2023.10223986.

[13] N. Karakullukcu and B. Yilmaz, "Detection of movement intention in EEG-Based Brain-Computer interfaces using Fourier-Based Synchrosqueezing Transform," *International Journal of Neural Systems*, vol. 32, no. 01, Nov. 2021. DOI: 10.1142/s0129065721500593. [Online]. Available: https://doi.org/10.1142/s0129065721500593.

[14] Y. Wang, Y. Bai, X. Xia, *et al.*, "Comparison of synchrosqueezing transform to alternative methods for time-frequency analysis of TMS-evoked EEG oscillations," *Biomedical Signal Processing and Control*, vol. 70, p. 102 975, Jul. 2021. DOI: 10.1016/j.bspc.2021.102975. [Online]. Available: https://doi.org/10.1016/j.bspc.2021.102975.

[15] O. K. Cura and A. Akan, "Classification of epileptic EEG signals using synchrosqueezing transform and machine learning," *International Journal of Neural Systems*, vol. 31, no. 05, p. 2 150 005, Nov. 2020. DOI: 10.1142/s0129065721500052. [Online]. Available: https://doi.org/10.1142/s0129065721500052.

[16] M. A. Ozdemir, O. K. Cura, and A. Akan, "Epileptic EEG classification by using Time-Frequency images for deep learning," *International Journal of Neural Systems*, vol. 31, no. 08, p. 2 150 026, May 2021. DOI: 10.1142/s012906572150026x. [Online]. Available: https://doi.org/10.1142/s012906572150026x.

[17] M. Amiri, H. Aghaeinia, and H. R. Amindavar, "Automatic epileptic seizure detection in EEG signals using sparse common spatial pattern and adaptive short-time Fourier transform-based synchrosqueezing transform," *Biomedical Signal Processing and Control*, vol. 79, p. 104 022, Aug. 2022. DOI: 10.1016/j.bspc.2022.104022. [Online]. Available: https://doi.org/10.1016/j.bspc.2022.104022.

[18] E. Marchi, M. Cervetto, and C. Galarza, "Adaptive synchrosqueezing wavelet transform for real-time applications," *Digital Signal Processing*, vol. 140, p. 104 133, Jun. 2023. DOI: 10.1016/j.dsp.2023.104133. [Online]. Available: https://doi.org/10.1016/j.dsp.2023.104133.

[19] "Epileptic seizure recognition." (Oct. 11, 2018), [Online]. Available: https://www.kaggle.com/datasets/harunshimanto/epileptic-seizure-recognition.

[20] R. G. Andrzejak, K. Lehnertz, F. Mormann, C. Rieke, P. David, and C. E. Elger, "Indications of nonlinear deterministic and finite-dimensional structures in time series of brain electrical activity: Dependence on recording region and brain state," *Physical review. E, Statistical physics, plasmas, fluids, and related interdisciplinary topics*, vol. 64, no. 6, Nov. 2001. DOI: 10.1103/physreve.64.061907. [Online]. Available: https://doi.org/10.1103/physreve.64.061907.

[21] Edgardomarchi, *GitHub - edgardomarchi/adaptivesswt: Implementation of adaptive synchrosqueezing wavelet transform*. [Online]. Available: https://github.com/edgardomarchi/adaptivesswt.

[22] P. Virtanen, R. Gommers, T. E. Oliphant, *et al.*, "SciPy 1.0: Fundamental Algorithms for Scientific Computing in Python," *Nature Methods*, vol. 17, pp. 261–272, 2020. DOI: 10.1038/s41592-019-0686-2.

[23] F. Pedregosa, G. Varoquaux, A. Gramfort, *et al.*, "Scikit-learn: Machine learning in Python," *Journal of Machine Learning Research*, vol. 12, pp. 2825–2830, 2011.

[24] J. D. Hunter, "Matplotlib: A 2d graphics environment," *Computing in Science & Engineering*, vol. 9, no. 3, pp. 90–95, 2007. DOI: 10.1109/MCSE.2007.55.

[25] M. L. Waskom, "Seaborn: Statistical data visualization," *Journal of Open Source Software*, vol. 6, no. 60, p. 3021, 2021. DOI: 10.21105/joss.03021. [Online]. Available: https://doi.org/10.21105/joss.03021.

[26] N. V. Chawla, K. W. Bowyer, L. O. Hall, and W. P. Kegelmeyer, "SMOTE: Synthetic Minority Over-sampling technique," *Journal of Artificial Intelligence Research*, vol. 16, pp. 321–357, Jun. 2002. DOI: 10.1613/jair.953. [Online]. Available: https://doi.org/10.1613/jair.953.

[27] L. Li, H. Cai, and Q. Jiang, "Adaptive synchrosqueezing transform with a time-varying parameter for non-stationary signal separation," *Applied and Computational Harmonic Analysis*, vol. 49, no. 3, pp. 1075–1106, Jul. 2019. DOI: 10.1016/j.acha.2019.06.002. [Online]. Available: https://doi.org/10.1016/j.acha.2019.06.002.

[28] H. Kode, K. Elleithy, and L. Almazaydeh, "Epileptic seizure detection in EEG signals using machine learning and deep learning techniques," *IEEE Access*, vol. 12, pp. 80 657–80 668, Jan. 2024. DOI: 10.1109/access.2024.3409581. [Online]. Available: https://doi.org/10.1109/access.2024.3409581.

[29] U. Ayman, M. S. Zia, O. D. Okon, *et al.*, "Epileptic Patient Activity Recognition System using Extreme Learning Machine method," *Biomedicines*, vol. 11, no. 3, p. 816, Mar. 2023. DOI: 10.3390/biomedicines11030816. [Online]. Available: https://doi.org/10.3390/biomedicines11030816.

[30] P. Kunekar, M. K. Gupta, and P. Gaur, "Detection of epileptic seizure in EEG signals using machine learning and deep learning techniques," *Journal of Engineering and Applied Science*, vol. 71, no. 1, Jan. 2024. DOI: 10.1186/s44147-023-00353-y. [Online]. Available: https://doi.org/10.1186/s44147-023-00353-y.